ACS APPLIED MATERIALS & INTERFACES

Research Article

www.acsami.org

Band-Selective Coupling-Induced Enhancement of Two-Photon Photoluminescence in Gold Nanocubes and Its Application as Turn-on Fluorescent Probes for Cysteine and Glutathione

Zhenping Guan, Shuang Li, Pei Boon Stephanie Cheng, Na Zhou, Nengyue Gao, and Qing-Hua Xu*

Department of Chemistry, National University of Singapore, 3 Science Drive 3, Republic of Singapore 117543

Supporting Information

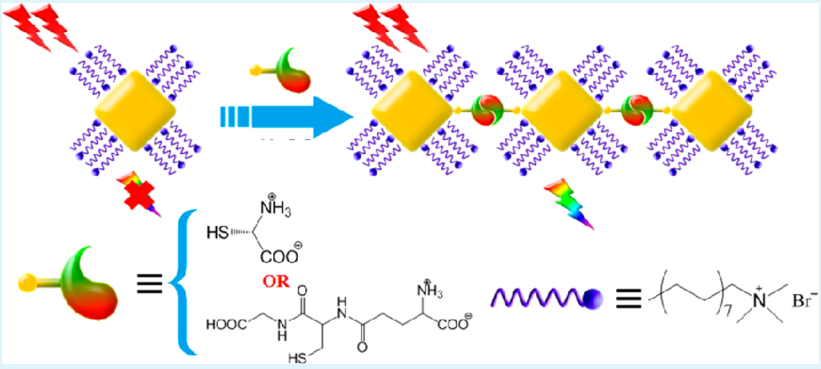

ABSTRACT: We have demonstrated that cysteine and glutathione induced edge-to-edge coupling of gold nanocubes (Au NCs) caused a band-selective enhancement of two-photon photoluminescence (TPPL). The photoluminescence intensity of the X-band of Au NCs was found to be enhanced up to 60-fold and 46-fold upon addition of cysteine and glutathione, respectively, while the intensity of L-band remained almost unchanged. This band-selective enhancement behavior is totally different from the previously observed aggregation enhanced TPPL of spherical metal nanoparticles (NPs). The band-selective enhancement was ascribed to preferential enhancement of the X-band emission through resonant coupling with longitudinal surface plasmon resonance (SPR) band of the Au NCs assembly. This phenomenon was utilized to develop a new two-photon fluorescence turn-on sensing platform for detection of cysteine and glutathione. This method displayed high sensitivity and excellent selectivity over the other 19 amino acids. Together with the advantage of deep tissue penetration and localized excitation of two-photon near-infrared excitation, this strategy has promising applications in in vivo biosensing and imaging.

KEYWORDS: *Au nanoparticles, surface plasmon resonance, plasmon coupling, two-photon photoluminescence, fluorescence enhancement, biosensing*

INTRODUCTION

Noble-metal nanoparticles (NPs), such as Au and Ag, display a unique optical property known as surface plasmon resonance (SPR), which arises from the collective oscillation of the conduction-band electrons.[1−3] The SPR band is sensitive to the particle size, shape, and dielectric properties of the media surrounding the metal nanoparticles.[2,4,5] Plasmon coupling of closely spaced metal nanoparticles can also lead to a red-shifted SPR peak[6−9] and significantly enhanced local electrical field within the gap region.[10] The field enhancement can amplify both the incoming and outgoing light fields and, consequently, increase the excitation efficiency and radiative decay rates.[11] Interactions between noble-metal NPs and chromophores are responsible for many interesting phenomena such as surface-enhanced Raman scattering (SERS), metal-enhanced fluorescence, second-harmonic generation (SHG), and two-photon photoluminescence (TPPL).[12−17] These phenomena have been widely utilized in various applications such as sensing, imaging, and optoelectronics.[18−20]

As one of the 20 most important amino acids encoded by the universal genetic code, cysteine plays a crucial role in the physiological processes of human body by providing intramolecular cross-linking of protein through disulfide bonds to support their secondary structures and functions.[21] A deficiency of cysteine would lead to many diseases, such as hematopoiesis decrease, leukocyte loss, and psoriasis.[22] Glutathione is another very important thiol species abundant in cells with vital biological functions. It keeps the cysteine thiol groups of proteins in the reduced state and protects DNA and RNA from oxidation.[23] Therefore, it is important to detect cysteine and glutathione in vivo with high sensitivity. Various methods,

Received: August 29, 2012
Accepted: October 4, 2012
Published: October 4, 2012

including fluorescent dye-based fluorometry,[24] electrochemical voltammetry,[22] and fluorescence-coupled high-performance liquid chromatography (HPLC) techniques,[25] have been developed for detection of cysteine and glutathione. Cysteine and glutathione molecules were found to induce particle aggregation of metal nanoparticles, resulting in a red-shift of their SPR bands.[6−8] This phenomenon has been utilized to develop colorimetric assays for detection of cysteine and glutathione. The colorimetric methods generally gave limited sensitivity with limit of detection (LOD) of ≥5 μM.[7,8]

Emission methods usually offer higher sensitivity, compared to the colorimetric methods. However, noble-metal NPs generally display low emission quantum yields.[26] Two mechanisms were proposed to account for the photoluminescence in Au nanostructures: interband transition and plasmonic emission. The interband emission originates from the recombination of sp-band electrons with d-band holes, which preferentially occurs near the L and X symmetry points of the Brillouin zone of a face-centered cubic (fcc) gold crystal structure and gives emission bands at 510 and 630 nm, respectively.[27,28] The plasmonic emission arises from direct radiative relaxation of surface plasmon. The resultant emission spectra closely resemble their extinction spectra.[29,30] Both emission processes can be significantly affected by the local field enhancement of the metal NPs. Recently, we found that aggregation-induced plasmon coupling can cause significantly enhanced TPPL of metal NPs (by up to 50-fold).[16] The plasmon-coupling-induced TPPL enhancement has been further utilized to develop a new sensing platform for Hg^{2+} detection with significantly improved sensitivity and selectivity, compared to the colorimetric approach.[31] Compared to silver (Ag) NPs, gold (Au) NPs are known to display better biocompatibility.[18,19] We have recently demonstrated that coupled Au NPs displayed TPPL enhancement comparable to that of Ag.[32] Gold nanocubes (Au NCs) have been found to display higher emission quantum efficiency than metal NPs of other shapes.[33] Here, we demonstrate that cysteine/glutathione can induce TPPL enhancement of Au NCs. Au NCs thus can act as a cysteine/glutathione probe. This method displays high sensitivity and excellent selectivity over the other 19 amino acids. In addition, using near-infrared (NIR) light as the excitation source, two-photon excitation possesses the advantages of high penetration depth, intrinsically localized excitation, less tissue autofluorescence, and reduced photodamage. This new approach has promising applications in in vivo biosensing and imaging.

EXPERIMENTAL SECTION

Materials. Gold(III) chloride trihydrate ($HAuCl_4·3H_2O$, 99.9%), sodium borohydride ($NaBH_4$, 98%), L-alanine (Ala), L-arginine (Arg), L-asparagine (Asn), L-aspartic acid (Asp), L-cysteine (Cys), L-glutamic acid (Glu), L-glutamine (Gln), L-glutathione (GSH), glycine (Gly), L-histidine (His), L-isoleucine (Ile), L-leucine (Leu), L-lysine (Lys), L-methionine (Met), L-phenylalanine (Phe), L-proline (Pro), L-serine (Ser), L-threonine (Thr), L-tryptophan (Trp), L-tyrosine (Try), and L-valine (Val) were purchased from Sigma−Aldrich. Cetyltrimethylammonium bromide (CTAB) and L-(+)-ascorbic acid (99%) were purchased from Alfa Aesar. All chemicals were used as-received, without further purification. All aqueous solutions are prepared in deionized (DI) water.

Preparation of Gold Nanocubes (Au NCs). Au NCs were prepared using a previously reported seed-mediated method.[34] The seeds were prepared by sequential addition of $HAuCl_4$ (0.125 mL, 0.01 M) and freshly prepared ice-cold $NaBH_4$ solution (0.3 mL, 0.01 M) into CTAB aqueous solution (3.75 mL, 0.1 M), followed by rapid stirring for 2 min. The resultant seed solution was kept at room temperature for 1 h prior to use. The growth solution was prepared by sequential addition of CTAB (6.4 mL, 0.1 M), $HAuCl_4$ (0.8 mL, 0.01 M) and ascorbic acid (3.8 mL, 0.1 M) into water (32 mL). The seed solution was diluted 10 times in water. 0.02 mL of diluted seed solution was then added into the growth solution. The resultant solution was mixed by gentle inversion for 10 s and then left undisturbed overnight.

Sample Preparation for Amino Acid Sensing. The pH of the as-prepared Au NCs was first adjusted to 2.3 by adding the proper amount of 1.0 M HCl. Proper amounts of 0.1 M cysteine and glutathione stock solutions were then added into 2 mL of Au NCs. For other amino acids, 150 μM was added to the Au NCs solution. The samples were incubated at 35 °C for 10 min before the measurements.

Instrumentations and Characterizations. The pH value was measured using a MP220 pH meter. Transmission electron microscopy (TEM) images of nanoparticles were obtained using a Philips CM10 TEM microscope at an accelerating voltage of 100 kV. Ultraviolet−visible light (UV-vis) extinction spectra were measured using a Shimadzu Model UV-2550 spectrophotometer. One-photon photoluminescence was measured using a 10-mW 405-nm diode laser as the excitation source. Two-photon photoluminescence was measured using a mode-locked femtosecond Ti:sapphire oscillator (Tsunami, Spectra Physics) as the excitation source. The output laser pulses have a central wavelength at 820 nm with pulse duration of ~80 fs and repetition rate of 80 MHz. The laser power for two-photon excitation before the sample was 100 mW. The laser beam was focused onto the sample using a lens with focus length of 3 cm. The emission from the sample was collected at the perpendicular direction of the excitation beam to minimize the scattering and directed into a monochromator (Acton, Spectra Pro 2300i) coupled CCD (Princeton Instruments, Pixis 100B), using an optical fiber. A 450-nm long-pass and a 750-nm short-pass filter was placed before the monochromator for one-photon and two-photon excitation, respectively, to minimize the light scattering from the excitation beam.

RESULTS AND DISCUSSION

Cysteine-/Gutathione-Induced Assembly of Au NCs. As thiol-containing amino acids, cysteine and glutathione can easily bind to the surface of Au NPs.[35,36] In the acidic environment, their carboxyl and amino groups are ionized to form a zwitterionic structure (see Scheme 1). The cooperative two-point electrostatic interaction induces the coupling of Ag and Au NPs.[35,36]

The morphology of the prepared Au NCs was confirmed by their TEM images (Figure 1A). The isolated Au NCs have an

Scheme 1. Assembly Mechanism of Gold Nanocubes (Au NCs) Induced by Cysteine/Glutathione

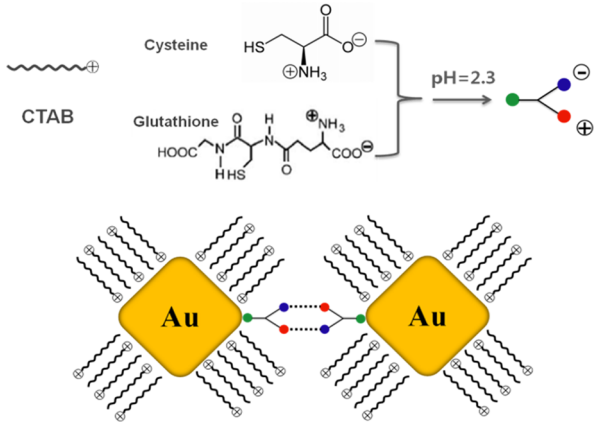

dx.doi.org/10.1021/am301822v | ACS Appl. Mater. Interfaces 2012, 4, 5711−5716

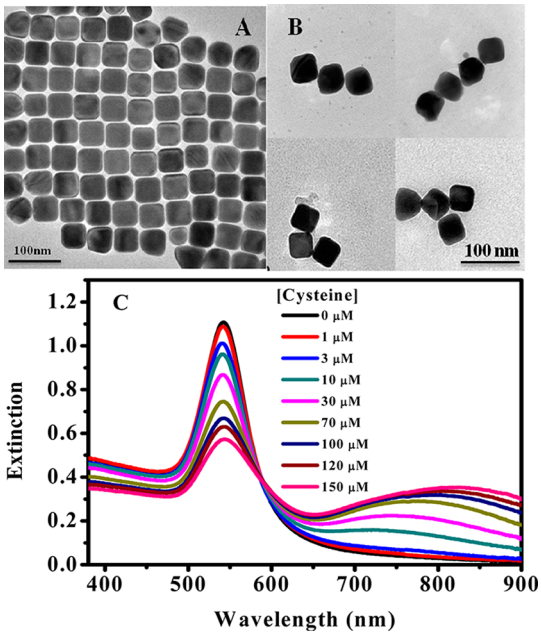

Figure 1. (A, B) TEM images of isolated Au NCs (panel A) and coupled Au NCs (panel B) in the presence of 100 μM cysteine. (C) Extinction spectra of Au NCs solution (pH 2.3, T = 35 °C) before and after the addition of cysteine.

average edge length of 40 nm. Cysteine-induced assembly of Au NCs was confirmed by their TEM images (Figure 1B) and UV–vis extinction spectra (Figure 1C). The extinction spectrum of Au NCs solution displayed a characteristic plasmon band peaking at 544 nm. Upon addition of cysteine, the intensity of the original SPR band at 544 nm decreased and a new band appeared at the longer wavelength region. This new band is a typical feature of longitudinal plasmon mode along the axis of coupled metal nanoparticles. The result is consistent with the previous reports and plasmon hybridization model,[37−39] indicating the formation of an Au NC assembly. When more cysteine was added, this new band further red-shifted gradually and its intensity steadily increased, indicating increased chain length. Similar effect was also observed by adding glutathione to the Au NC solution (see the Electronic Supporting Information (ESI)). The coupling of Au NCs can be directly visualized by the TEM images (Figure 1B). Upon the addition of cysteine, Au NCs form chainlike structures with a dominant edge-to-edge coupling orientation. It has been previously reported that the as-prepared Au NCs were stabilized by a positively charged CTAB bilayer that is less ordered at the curved edges than on the smooth surfaces of Au NCs, allowing thiol-containing species to bind preferentially to the edge area and form an edge-to-edge particle assembly (see Scheme 1).[34,35]

One-Photon Photoluminescence of Coupled NCs. The one-photon photoluminescence spectra of isolated and coupled Au NCs were measured using a 405-nm diode laser as the excitation source, and the results are shown in Figure 2. Two emission peaks at ~510 and ~620 nm were clearly observed, implying an emission mechanism of interband transition instead of plasmonic emission, as the spectra of plasmonic emission usually closely resembling that of SPR. These two peaks were thus assigned to the radiative relaxation of the L- and X-bands, respectively. The emission slightly decreased upon the addition of cysteine (Figure 2), which is mainly due to

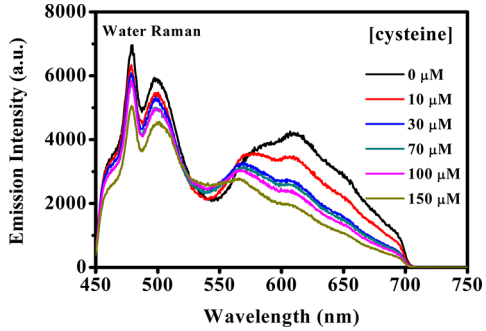

Figure 2. One-photon photoluminescence of Au NCs solution acquired 10 min after the addition of cysteine (pH 2.3, T = 35 °C, λ_{EX} = 405 nm).

the decreasing absorbance at the excitation wavelength (405 nm) upon the assembly (Figure 1C).[40] The subtle change in the shape of emission spectra upon addition of cysteine is also related to the change in the extinction spectra. The emission at the longer wavelength portion is attenuated by reabsorption more than the shorter wavelength portion, because of increased extinction at longer wavelength of the assembled structures.

Cysteine-/Glutathione-Induced Two-Photon Photoluminescence Enhancement. The two-photon photoluminescence of the isolated and assembled Au NCs was measured using femtosecond laser pulses with a central wavelength at 820 nm as the excitation source. The results under two-photon excitation (Figure 3) are strikingly different from those under one-photon excitation (Figure 2). Under two-photon excitation, only very weak emission was observed in the isolated Au NCs solution (Figure 3). Upon addition of cysteine, the longer wavelength component (centered at ~650 nm, X-band emission) was significantly enhanced and steadily increased until [cysteine] reached 150 μM (Figure 3). The emission intensity at 650 nm increased by up to 60 times. The X-band emission was also significantly enhanced in the presence of glutathione with enhancement factor of up to 46 folds (Figure S2 in the ESI). The shorter-wavelength component (centered at ~520 nm, L-band) only displayed minor enhancement, primarily because of overlapping with the tail of the enhanced longer wavelength component (X-band, Figure S3 in the ESI). The two-photon excitation nature of the emission was confirmed by measuring its excitation power dependence for the coupled Au NC solution (Figure 3B). The log–log plot of the emission intensity at 650 nm versus excitation power (Figure 3B, inset) gave a slope of 2.1, confirming that the emission indeed arises from two-photon excitation.

The observed coupling-induced TPPL enhancement offers an excellent platform for detection of cysteine and glutathione. The enhancement factor of X-band emission was plotted with respect to [cysteine] and [glutathione], respectively (Figure 4). The inset shows TPPL enhancement factor is linearly proportional to the concentration of cysteine or glutathione in the low concentration range. The limit of detection (LOD) was estimated to be 0.5 μM for cysteine and 1.3 μM for glutathione, an improved sensitivity compared to the colorimetric method, which gave a LOD of 10 μM, as reported by Zhong et al.[7] The sensitivity is also better than the reported fluorescent-dye-based fluorometric assay (LOD of 5 μM)[24] and comparable to electrochemical voltammetry technique (LOD of 1 μM).[22]

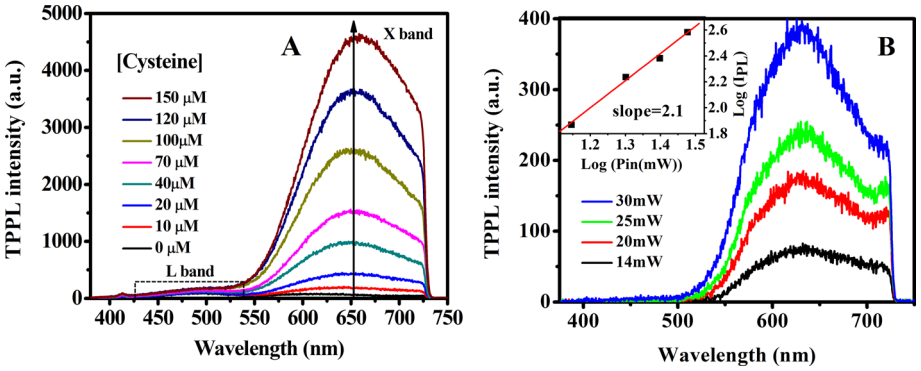

Figure 3. (A) TPPL spectra of Au NCs solution upon addition of cysteine. The excitation power is 100 mW. (B) Power dependence of TPPL e at 650 nm of Au NCs in the presence of 100 μM cysteine.

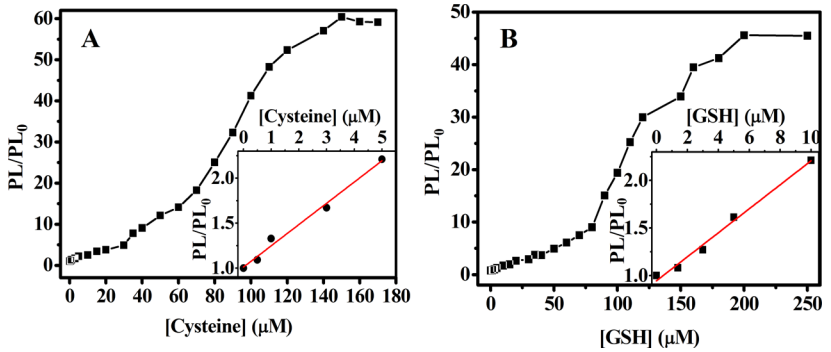

Figure 4. Plot of TPPL enhancement of X-band emission versus (A) [cysteine] and (B) [glutathione]. The inset shows that TPPL enhancement factor is linearly proportional to [cysteine] and [glutathione] in the low concentration range.

This sensing scheme also displays high selectivity for cysteine and glutathione. Figure 5 shows TPPL spectra after the addition of 150 μM of different common amino acids. The corresponding extinction spectra are shown in Figure S4 in the ESI. Only cysteine and glutathione displayed significant TPPL enhancement, while the other amino acids did not show observable enhancement. This result indicates that this two-photon photoluminescence method has high selectivity in discriminating cysteine and glutathione from other amino acids. Other amino acids do not have thiol groups and cannot induce the plasmon coupling, as evidenced by lack of a red-shift in their extinction spectra compared to the blank samples (see Figures S4 and S5 in the ESI). Experiments done at a lower concentration (3 μM) of amino acids (Figure S5 in the ESI) indicate that two-photon photoluminescence methods have better selectivity, compared to the colorimetric methods. However, considering the mild toxicity of CTAB-capped Au NPs[41,42] and the overall neutral pH environment of the human body, except some special organs (such as the stomach), the application of this method will be restricted to some special circumstances.

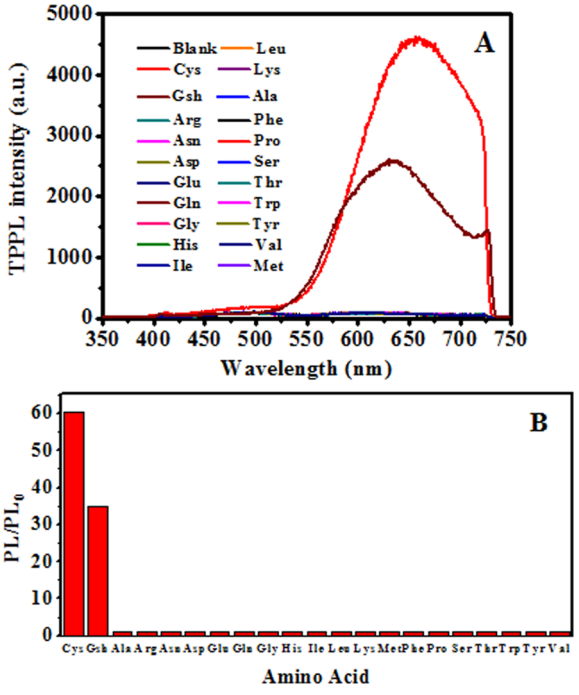

Figure 5. (A) TPPL spectra and (B) enhancement factor at 650 nm for coupled Au NCs in the presence of various amino acids. [amino acid] = 150 μM.

The TPPL Enhancement Mechanism. The observed huge TPPL enhancement could be ascribed to two effects. First, the formation of a chainlike structure in the coupled Au NCs resulted in the formation of a longitudinal mode in the 650–1000 nm region and, consequently, increased extinction at the excitation wavelength (820 nm). This new longitudinal band provides intermediate states to enhance two-photon excitation processes. On the other hand, the enhanced local electric field near the excitation wavelength also contributes to the enhanced TPPL. The chainlike structure and the SPR band of the coupled Au NCs resembles those of gold nanorods (Au NRs). Au NRs have longitudinal bands in the NIR region. It has been proposed that two-photon excitation of Au NRs was initiated

by the sequential absorption of two photons one by one.[43,44] The longitudinal band in the NIR range provides intermediate states to foster two-photon absorption processes. The strong TPPL of Au NRs were largely ascribed to strong local electric fields at the excitation wavelength.[45] The SPR amplitude at 820 nm (excitation wavelength) increased as the degree of coupling increased. Therefore, the enhanced local field gives rise to dramatic TPPL enhancement in the coupled Au NCs solution. Furthermore, the plasmon coupling will cause a dynamical charge redistribution with concentrated charges at the gap region[15] could further enhance the local-field intensity, especially for the resonators with sharp-tip or edge-directed coupling orientation.[30,46,47] In the current work, Au NCs were assembled preferentially with sharp edge-to-edge directed coupling orientation, which result in a huge enhancement of local field in the gap between the cube edges and also contribute to the observed TPPL enhancement.

In addition to intensity enhancement, it is interesting to note that plasmon coupling can also modulate spectral shape of TPPL of Au NCs. The TPPL spectral shape of Au NCs was found to be strongly dependent on the extent of coupling. The isolated and assembled Au NCs displayed totally different TPPL spectra (Figure 6). The L- and X-bands of the TPPL

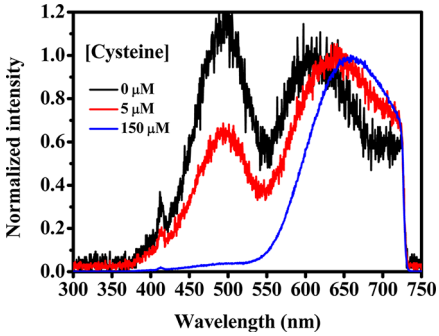

Figure 6. Normalized TPPL spectra of a gold nanocube (Au NCs) solution (pH 2.3) in the presence of 0, 5, and 150 μM cysteine.

spectra of isolated Au NCs have similar amplitudes. Upon the addition of cysteine and glutathione, the intensity of the X-band emission was dramatically enhanced, while the intensity of the L-band emission remained almost unchanged if the tail of the X-band emission is excluded (see Figure S1 in the ESI). This observation is different from the previous observation that the TPPL spectra of isolated and assembled spherical Au and Ag NPs remained almost unchanged.[16,31,32] The band-selective enhancement behavior can be explained as a consequence of preferential enhancement of the X-band emission through coupling with the longitudinal SPR mode of coupled particles. It has been reported that radiative transitions of fluorophores were strongly coupled with the SPR band of adjacent metal NPs.[48−51] Consequently, the emission was strongly polarized along the longitudinal SPR mode of metal NPs.[51] Previous single-particle studies on Au NRs revealed that emission from the X-band transition was highly polarized along the long axis of the rod, while the L-band emission did not show obvious polarization features.[43,52] The longitudinal SPR band of the coupled Au NC chains will be excited by the 820-nm fs laser pulses. The preferential coupling between the longitudinal plasmon with longer wavelength X-band transitions gives rise to a band-selective enhancement behavior.

CONCLUSION

We have demonstrated edge-to-edge coupling of gold nanocubes (Au NCs) induced by cysteine and glutathione, which caused a band-selective enhancement of two-photon photoluminescence. The X-band of two-photon photoluminescence (TPPL) of Au NCs was found to be enhanced up to 60-fold and 46-fold upon the addition of cysteine and glutathione, respectively, while the intensity of the L-band remained almost unchanged. The band-selective enhancement was ascribed to preferential enhancement of the X-band emission through resonant coupling with longitudinal SPR band of the Au NCs assembly. This phenomenon has been further utilized to develop a new two-photon sensing platform for detection of cysteine/glutathione. This method displayed high sensitivity and excellent selectivity over the other 19 amino acids. Together with the advantage of deep tissue penetration and localized excitation of two-photon near-IR excitation, this strategy has potential applications in the in vivo biosensing and bioimaging.

ASSOCIATED CONTENT

Supporting Information

Electronic supporting information (ESI) includes the following: extinction and two-photon emission spectra of a Au NC solution after the addition of glutathione; intensity change in the L-band of two-photon emission of a Au NC solution after the addition of cysteine; and UV−vis and TPPL spectra of Au NCs in the presence of various amino acids. This information is available free of charge via the Internet at http://pubs.acs.org/

AUTHOR INFORMATION

Corresponding Author

*E-mail: chmxqh@nus.edu.sg.

Notes

The authors declare no competing financial interest.

ACKNOWLEDGMENTS

We thank the financial support from DSTA Singapore (Project No. DSTA-NUS-DIRP/9010100347), the Singapore-MIT Alliance of Research and Technology (SMART) program under National Research Foundation Singapore and the Economic Development Board (SPORE, No. COY-15-EWI-RCFSA/N197-1).

REFERENCES

(1) Ehrenreich, H.; Philipp, H. R. *Phys. Rev.* **1962**, *128*, 1622−1629.
(2) Kelly, K. L.; Coronado, E.; Zhao, L. L.; Schatz, G. C. *J. Phys. Chem. B* **2003**, *107*, 668−677.
(3) Link, S.; El-Sayed, M. A. *J. Phys. Chem. B* **1999**, *103*, 8410−8426.
(4) Zhao, J.; Pinchuk, A. O.; McMahon, J. M.; Li, S.; Ausman, L. K.; Atkinson, A. L.; Schatz, G. C. *Acc. Chem. Res.* **2008**, *41*, 1710−1720.
(5) Noguez, C. *J. Phys. Chem. C* **2007**, *111*, 3806−3819.
(6) Sudeep, P. K.; Joseph, S. T. S.; Thomas, K. G. *J. Am. Chem. Soc.* **2005**, *127*, 6516−6517.
(7) Zhong, Z.; Patskovskyy, S.; Bouvrette, P.; Luong, J. H. T.; Gedanken, A. *J. Phys. Chem. B* **2004**, *108*, 4046−4052.
(8) Zhang, F. X.; Han, L.; Israel, L. B.; Daras, J. G.; Maye, M. M.; K. Ly, N.; Zhong, C.-J. *Analyst* **2002**, *127*, 462−465.
(9) Liu, D.; Wang, Z.; Jiang, X. *Nanoscale* **2011**, *3*, 1421−1433.
(10) Nie, S.; Emory, S. R. *Science* **1997**, *275*, 1102−1106.
(11) Mohamed, M. B.; Volkov, V.; Link, S.; El-Sayed, M. A. *Chem. Phys. Lett.* **2000**, *317*, 517−523.
(12) Camargo, P. H. C.; Rycenga, M.; Au, L.; Xia, Y. N. *Angew. Chem., Int. Ed.* **2009**, *48*, 2180−2184.

(13) Kinkhabwala, A.; Yu, Z.; Fan, S.; Avlasevich, Y.; Mullen, K.; Moerner, W. E. *Nat. Photon.* **2009**, *3*, 654−657.
(14) Jin, R.; Jureller, J. E.; Kim, H. Y.; Scherer, N. F. *J. Am. Chem. Soc.* **2005**, *127*, 12482−12483.
(15) Ghenuche, P.; Cherukulappurath, S.; Taminiau, T. H.; van Hulst, N. F.; Quidant, R. *Phys. Rev. Lett.* **2008**, *101*, 116805.
(16) Guan, Z.; Polavarapu, L.; Xu, Q.-H. *Langmuir* **2010**, *26*, 18020−18023.
(17) Polavarapu, L.; Xu, Q.-H. *Langmuir* **2008**, *24*, 10608−10611.
(18) Song, S.; Qin, Y.; He, Y.; Huang, Q.; Fan, C.; Chen, H.-Y. *Chem. Soc. Rev.* **2010**, *39*, 4234−4243.
(19) Saha, K.; Agasti, S. S.; Kim, C.; Li, X.; Rotello, V. M. *Chem. Rev.* **2012**, 2739−2779.
(20) Ray, P. C. *Chem. Rev.* **2010**, *110*, 5332−5365.
(21) Wood, Z. A.; Schröder, E.; Robin Harris, J.; Poole, L. B. *Trends Biochem. Sci.* **2003**, *28*, 32−40.
(22) Shahrokhian, S. *Anal. Chem.* **2001**, *73*, 5972−5978.
(23) Schafer, F. Q.; Buettner, G. R. *Free Radic. Biol. Med.* **2001**, *30*, 1191−1212.
(24) Zhang, M.; Yu, M.; Li, F.; Zhu, M.; Li, M.; Gao, Y.; Li, L.; Liu, Z.; Zhang, J.; Zhang, D.; Yi, T.; Huang, C. *J. Am. Chem. Soc.* **2007**, *129*, 10322−10323.
(25) Tcherkas, Y. V.; Denisenko, A. D. *J. Chromatogr. A* **2001**, *913*, 309−313.
(26) Dulkeith, E.; Niedereichholz, T.; Klar, T. A.; Feldmann, J.; von Plessen, G.; Gittins, D. I.; Mayya, K. S.; Caruso, F. *Phys. Rev. B* **2004**, *70*, 205424.
(27) Guerrisi, M.; Rosei, R.; Winsemius, P. *Phys. Rev. B* **1975**, *12*, 557−563.
(28) Beversluis, M. R.; Bouhelier, A.; Novotny, L. *Phys. Rev. B* **2003**, *68*, 115433.
(29) Bouhelier, A.; Bachelot, R.; Lerondel, G.; Kostcheev, S.; Royer, P.; Wiederrecht, G. P. *Phys. Rev. Lett.* **2005**, *95*, 267405.
(30) Wissert, M. D.; Ilin, K. S.; Siegel, M.; Lemmer, U.; Eisler, H.-J. *Nano Lett.* **2010**, *10*, 4161−4165.
(31) Jiang, C.; Guan, Z.; Rachel Lim, S. Y.; Polavarapu, L.; Xu, Q.-H. *Nanoscale* **2011**, *3*, 3316−3320.
(32) Han, F.; Guan, Z.; Tan, T. S.; Xu, Q.-H. *ACS Appl. Mater. Interfaces* **2012**, *4*, 4746−4751.
(33) Wu, X.; Ming, T.; Wang, X.; Wang, P.; Wang, J.; Chen, J. *ACS Nano* **2009**, *4*, 113−120.
(34) Kou, X. S.; Sun, Z. H.; Yang, Z.; Chen, H. J.; Wang, J. F. *Langmuir* **2009**, *25*, 1692−1698.
(35) Zhang, S.; Kou, X.; Yang, Z.; Shi, Q.; Stucky, G. D.; Sun, L.; Wang, J.; Yan, C. *Chem. Commun.* **2007**, 1816−1818.
(36) Sun, Z.; Ni, W.; Yang, Z.; Kou, X.; Li, L.; Wang, J. *Small* **2008**, *4*, 1287−1292.
(37) Nordlander, P.; Oubre, C.; Prodan, E.; Li, K.; Stockman, M. I. *Nano Lett.* **2004**, *4*, 899−903.
(38) Barrow, S. J.; Funston, A. M.; Gómez, D. E.; Davis, T. J.; Mulvaney, P. *Nano Lett.* **2011**, *11*, 4180−4187.
(39) Marhaba, S.; Bachelier, G.; Bonnet, C.; Broyer, M.; Cottancin, E.; Grillet, N.; Lermé, J.; Vialle, J.-L.; Pellarin, M. *J. Phys. Chem. C* **2009**, *113*, 4349−4356.
(40) Boyd, G. T.; Yu, Z. H.; Shen, Y. R. *Phys. Rev. B* **1986**, *33*, 7923−7936.
(41) Murphy, C. J.; Gole, A. M.; Stone, J. W.; Sisco, P. N.; Alkilany, A. M.; Goldsmith, E. C.; Baxter, S. C. *Acc. Chem. Res.* **2008**, *41*, 1721−1730.
(42) Patra, H. K.; Banerjee, S.; Chaudhuri, U.; Lahiri, P.; Dasgupta, A. K. *Nanomed.-Nanotechnol.* **2007**, *3*, 111−119.
(43) Imura, K.; Nagahara, T.; Okamoto, H. *J. Phys. Chem. B* **2005**, *109*, 13214−13220.
(44) Biagioni, P.; Celebrano, M.; Savoini, M.; Grancini, G.; Brida, D.; Mátéfi-Tempfli, S.; Mátéfi-Tempfli, M.; Duò, L.; Hecht, B.; Cerullo, G.; Finazzi, M. *Phys. Rev. B* **2009**, *80*, 045411.
(45) Wang, H.; Huff, T. B.; Zweifel, D. A.; He, W.; Low, P. S.; Wei, A.; Cheng, J.-X. *Proc. Natl. Acad. Sci. U.S.A.* **2005**, *102*, 15752−15756.
(46) Mühlschlegel, P.; Eisler, H.-J.; Martin, O. J. F.; Hecht, B.; Pohl, D. W. *Science* **2005**, *308*, 1607−1609.
(47) Schuck, P. J.; Fromm, D. P.; Sundaramurthy, A.; Kino, G. S.; Moerner, W. E. *Phys. Rev. Lett.* **2005**, *94*, 017402.
(48) Ringler, M.; Schwemer, A.; Wunderlich, M.; Nichtl, A.; Kurzinger, K.; Klar, T. A.; Feldmann, J. *Phys. Rev. Lett.* **2008**, *100*, 203002.
(49) Suzuki, M.; Yokoyama, H.; Brorson, S. D.; Ippen, E. P. *Appl. Phys. Lett.* **1991**, *58*, 998−1000.
(50) Zhao, L.; Ming, T.; Chen, H.; Liang, Y.; Wang, J. *Nanoscale* **2011**, *3*, 3849−3859.
(51) Ming, T.; Zhao, L.; Chen, H.; Woo, K. C.; Wang, J.; Lin, H.-Q. *Nano Lett.* **2011**, *11*, 2296−2303.
(52) Imura, K.; Nagahara, T.; Okamoto, H. *J. Am. Chem. Soc.* **2004**, *126*, 12730−12731.